

Beam-Sweep Magnet With Rotating Dipole Field

F. M. Bieniosek
21-June-1996

The concept of a rotating field holds a number of advantages for a beam sweeping system. However, it had not previously been considered a serious possibility because of the practical impossibility of creating a rotating field with sufficient field uniformity with a reasonable number of power supplies. This note proposes a method of generating such a field with two or three power supplies. Four (or six) conductors are driven in pairs. Although the field at any given slice of the magnet is not uniform, it is possible to twist the conductors such that the line integral of the transverse magnetic field along the path of the beam is uniform and rotating. The conductors can also be placed such that magnetic coupling between the circuits is negligible, which is important if the power supplies are to operate properly.

Rotating Field.

The magnetic field due to two pairs of current-carrying conductors oriented 90 degrees apart on a circle of radius r surrounding the beam is a dipole field, with strength

$$\vec{B}_0 = \frac{\mu_0 I_0}{\pi r} (\sin \omega t \hat{x} + \cos \omega t \hat{y})$$

if the current through the horizontal and vertical pairs are $I_0 \cos \omega t$ and $I_0 \sin \omega t$ respectively. The strength of the magnetic field on axis is constant and rotates azimuthally as a function of time with period $t = 2\pi / \omega$. A magnetic core amplifies the field by providing a return path for the magnetic field. However the field distribution is not sufficiently uniform for use as a sweep magnet (see Fig. 1).

If the current in the two phases is distributed as $\cos \theta$ and $\sin \theta$ respectively, the current distribution becomes

$$\begin{aligned}
I(\theta, t) &= I_0 (\cos \theta \cos \omega t + \sin \theta \sin \omega t) \\
&= I_0 \cos(\omega t - \theta)
\end{aligned} \tag{1}$$

i.e. the current distribution is rotating. This current distribution provides a uniform rotating dipole field.

Similarly, if three phases are available and the currents are distributed as $\cos \theta$, $\cos(\theta + 2\pi/3)$, $\cos(\theta - 2\pi/3)$, the current distribution becomes

$$\begin{aligned}
I(\theta, t) &= I_0 [\cos \theta \cos \omega t + \cos(\theta + 2\pi/3) \cos(\omega t + 2\pi/3) + \cos(\theta - 2\pi/3) \cos(\omega t - 2\pi/3)] \\
&= \frac{3}{2} I_0 \cos(\omega t - \theta)
\end{aligned} \tag{2}$$

which is again a rotating current distribution. The three-phase magnet is described below, after the two phase magnet.

Twisted Field Coils.

It is not possible to distribute the currents as $\cos \theta$ and $\sin \theta$ for a single-turn magnet. But one may synthesize such a field distribution in several different ways. The conventional approach to sweeping the beam is to synthesize a rotating magnetic field by two orthogonal linear “kickers” each excited in quadrature by a sinusoidal current. This approach, although simple, has the disadvantage that by splitting the sweep magnet into two parts, peak electric and magnetic fields must be doubled, since each half-magnet must provide the entire field at some part of the cycle. There is no particular reason why the field must be split into two halves. Here we explore the possibility of synthesizing the rotating field in a single magnet by twisting the conductors such that the axial current distribution integrated over the length of the magnet has the $I_0 \sin(\omega t - \theta)$ distribution. Suppose that the shape of the conductor is $z = z_0 \sin \theta$ where z_0 is an axial length (for example, half the length of the magnet). Then the current in the z -direction is $j_z = j_0 \sin \psi$ where $\tan \psi = dz / d(r\theta) = z_0 / r_0 \cos \theta$ is the slope of the conductor. Then

$$\sin \psi = \frac{\tan \psi}{\sqrt{1 + \tan^2 \psi}} = \frac{z_0}{r_0} \frac{\cos \theta}{\sqrt{1 + (z_0 / r_0 \cos \theta)^2}} \tag{3}$$

and the effect of a current element on the beam is $j_z(\theta) dz$ where $dz = z_0 \cos \theta d\theta$. Thus

$$j_z(\theta) dz = j_0 \frac{z_0^2}{r_0} \frac{\cos^2 \theta d\theta}{\sqrt{1 + (z_0 / r_0 \cos \theta)^2}} \approx j_0 z_0 \cos \theta d\theta \quad (4)$$

where the approximation is for $z_0/r_0 \gg 1$ (long, thin magnet). The magnetic field generated by such a distribution is

$$B_x z_0 = \frac{\mu_0}{2\pi r} \int_{-\pi/2}^{\pi/2} j_z(\theta) \cos \theta d\theta = \frac{\mu_0 j_0 z_0}{2\pi r} \int_{-\pi/2}^{\pi/2} \cos^2 \theta d\theta = \frac{\mu_0 j_0 z_0}{4r} \quad (5)$$

Since the total current in the distribution is

$$I_0 = \int_{-\pi/2}^{\pi/2} j_0 \cos \theta d\theta = 2j_0 \quad (6)$$

the penalty in field exacted for distributing the current azimuthally is the ratio

$$\frac{B_x(\cos \theta \text{ distribution})}{B_x(\text{filament})} = \frac{\pi}{4} \quad (7)$$

i.e. the current in the twisted conductor must be increased by the factor $4/\pi=1.273$ to produce the same field on axis as a single axial conductor. Detailed calculations for the general shape ($z_0/r_0 \sim 1$) remain to be completed.

The advantages of the single magnet with rotating field are:

1. Because the magnet is roughly twice as long as in the two-unit approach, the requirements on the deflecting magnetic field, the axial electric field, the fields in the core are all reduced.
2. End effects are less important in a single unit than in two units. In practice this means that the effective length of a single unit is more than twice that of two units.
3. A single unit makes mechanical construction and operation of the sweeping system simpler --for example, it is necessary to build only a single "universal" module.
4. The cylindrically-symmetric design lends itself naturally to tape-wound cores, which are by nature cylindrically symmetric. Because axial electric fields are reduced, it becomes easier to support these fields with a stack of tape-wound cores.

Expansion of Magnetic Field.

The transverse force on the beam is

$$\vec{F} = \beta c \int d\vec{z} \times \vec{B} \quad (8)$$

which, if the magnetic field \vec{H} can be expressed as the gradient of a scalar $\vec{H} = -\nabla\phi$, becomes

$$\vec{F} = -\mu_0\beta c \int d\vec{z} \times \nabla\phi = \mu_0\beta c \int \nabla_\tau \phi dz = \mu_0\beta c \nabla_\tau \int \phi dz \quad (9)$$

where the gradient is taken only in the transverse direction. The multipole expansion of the field can be found by considering the Dirichlet problem for a circle. For $\nabla^2\phi = 0$ and $\phi(r, \theta) = f(\theta)$, the solution to the problem is [Ref. 1]

$$\phi(r, \theta) = \frac{1}{2\pi} \int_0^{2\pi} \frac{1-\rho^2}{1-2\rho\cos(\theta-\tau)+\rho^2} f(\tau) d\tau \quad (10)$$

where ρ is the normalized radius. Defining

$$u(r, \theta) = \int \phi(r, \theta) dz$$

one has

$$u(r, \theta) = \frac{1}{2\pi} \int_0^{2\pi} \int \frac{1-\rho^2}{1-2\rho\cos(\theta-\tau)+\rho^2} f(\tau) d\tau dz = \frac{1}{2\pi} \int_0^{2\pi} \frac{1-\rho^2}{1-2\rho\cos(\theta-\tau)+\rho^2} \int f(\tau) dz d\tau \quad (11)$$

and, letting $g(\tau) = \int f(z, \tau) dz$, the expression becomes simply

$$u(r, \theta) = \frac{1}{2\pi} \int_0^{2\pi} \frac{1-\rho^2}{1-2\rho\cos(\theta-\tau)+\rho^2} g(\tau) d\tau \quad (12)$$

which has the same form as Eq. 10. Thus a solution for the line integral of the transverse magnetic field is mathematically equivalent to a solution for the local field.

If the integrated magnetic potential on the surface of the circle is expanded in a Fourier series in θ , where δ is an arbitrary angle offset,

$$g(\theta) = a_1 \cos\theta + a_2 \cos 2(\theta + \delta) + a_3 \cos 3(\theta + \delta) + \dots \quad (13)$$

then the integral has the following solution inside the circle.

$$u(r, \theta) = a_1 \rho \cos\theta + a_2 \rho^2 \cos 2(\theta + \delta) + a_3 \rho^3 \cos 3(\theta + \delta) + \dots \quad (14)$$

Differentiating to determine the line integral of the magnetic field H at the angles $\delta=0$ and $\delta=\pi$, the result is that the amplitudes of the dipole, quadrupole, and sextupole components are respectively

$$\begin{aligned} H_1 &= a_1 \\ H_2 &= 2a_2\rho \\ H_3 &= 3a_3(4\rho^2 - 1) \end{aligned} \tag{15}$$

If we want to keep the amplitude of each component below some fraction ϵ of the dipole field inside (say) $\rho=0.5$, the limits on the amplitudes of the higher order terms at the radius of the winding are $a_2 < 2\epsilon$, $a_3 < 4\epsilon$, ...

As an example, consider a set of coils which consist of a helical spiral wound around the cylinder with a pitch of 180° per winding. Then, at the instant at which the current is carried in only one pair of conductors, the current density distribution is a square wave, with Fourier components

$$f(\theta) = \frac{4}{\pi} \sin \theta + \frac{4}{3\pi} \sin 3\theta + \frac{4}{5\pi} \sin 5\theta + \dots \tag{16}$$

where the even-order terms are zero, and the worst case third order harmonic content inside the circle $\rho=0.5$ is 8.3% of the fundamental. This is somewhat larger than the field uniformity requirement for a sweep magnet (typically about 3%). At other moments in the cycle, the harmonic content of the current distribution and the field will vary as a function of time. Clearly the windings must follow a sine-wave shape more closely than the uniform helix.

A Practical 2-Phase Magnet.

Alternative designs for a set of field coils to be wrapped around a cylinder are indicated in Figures 2 and 3. The azimuthal angle around the cylinder is plotted in degrees, and the longitudinal distance z is in arbitrary units. A practical magnet will be much more elongated than implied by the drawings. The windings are in the form of squirrel cage (in analogy to the squirrel-cage rotor of an induction motor) twisted in the shape of $\cos \theta$ and $\sin \theta$, repeated symmetrically in z and θ . There are two circuits. The first circuit (black) has a current flowing at the instant pictured, indicated by the arrows, entering the magnet at $z=2$ at 180° (black circle) and leaving at 0° (or 360°). The current flows from the midplane to the ends of the magnet where it rotates 180° on end rings which are common to the two circuits, and returns to the midplane to the opposite terminal of the circuit. Each winding may twist a full 360° from end to end of the magnet (Fig. 2), or 180° to yield a simpler geometry (Fig. 3). The 180° option uses only the portion of the plot extending from $z=1$ to $z=3$, with end rings at these locations. The situation

pictured represents the current flow for a uniform horizontal integrated magnetic field, if $\theta=0$ corresponds to horizontal. As time progresses, the second circuit (gray) will begin to carry current, and the overall current distribution will rotate with time if the currents in the two circuits are properly phased. The windings are placed symmetrically at 90° intervals, such that magnetic coupling between the two circuits is zero. Since the power supplies for the two phases are bipolar, and the magnet is symmetric, the voltage at the ends of the magnet is always zero. Any imbalance in the voltage of one of the circuits couples into the other circuit only in the common mode; differential-mode coupling does not occur due to the end rings. Common-mode currents do not couple into the beam on average because of symmetry, and can be kept small by ensuring that the common mode impedance of the power supplies is larger than the differential mode impedance.

The twisted squirrel cage magnet driven by two bipolar supplies is relatively simple and mechanically robust. There are no breaks in the winding for power supply leads, and since the voltage at the ends is nominally zero, there is no need to allocate space to provide electrical insulation from neighboring devices in the target station. Each current path is the form of a distorted double helix; an attempt to provide a 3-D view of 360° magnet windings is shown in Figure 4.

Tape-wound magnetic cores will be used to provide a return path for the magnetic field, as shown in Figure 5. A typical path for current flow in the winding is indicated. The cores are all at ground potential and stacked with gaps to support the induced longitudinal electric field. If, for example, 1/2-inch cores are stacked with 1/4-inch gaps, a 50-cm-long magnet will have about 26 cores (13 on each side).

Because of the complicated shape of the magnetic field lines, which must be transverse to the beam, but twist around to be parallel to the direction of the magnetic tapes, a 3-D calculation of the magnetic field will be required to determine the precise voltage and current requirements for the magnet. An estimate may be developed from POISSON (Figure 1). Assume a downstream sweep magnet with an effective length (for calculating magnetic field) of 50 cm, a physical length (for calculating inductance) of 56 cm, a 5-mm diameter conductor on a winding radius of 16.5 mm, and inner radius of the core of 22.2 mm (1.75-inch ID). The antiprotons to be collected will remain inside a circle of 11-mm radius. These dimensions provide a 3-mm gap between the beam and the conductors, and a 3.2-mm gap between the core and the conductors, for a ceramic tube and a copper grounding/cooling strap for the cores. At 625 kHz the skin depth is small, and the conductors are modelled as flux excluders. The peak current is 2409 A per circuit for a required field on axis of 880 G. This field yields the same deflection as a 2000 G field in the "kicker" magnet design. The single-turn inductance calculated from the stored energy is $0.817 \mu\text{H}$. After accounting for the factor $4/\pi$ from the twist, and accounting for the fact that the magnet is effectively split into two halves, the power supply current and voltage are $I=6136 \text{ A}$, $V=4922 \text{ V}$. The peak voltage with respect to ground is $\pm 2.5 \text{ kV}$, and the peak voltage difference between neighboring

conductors is 3.5 kV. The conductors are electrically insulated from the cores by a ceramic tube, and from each other by the 18-mm air gap between conductors.

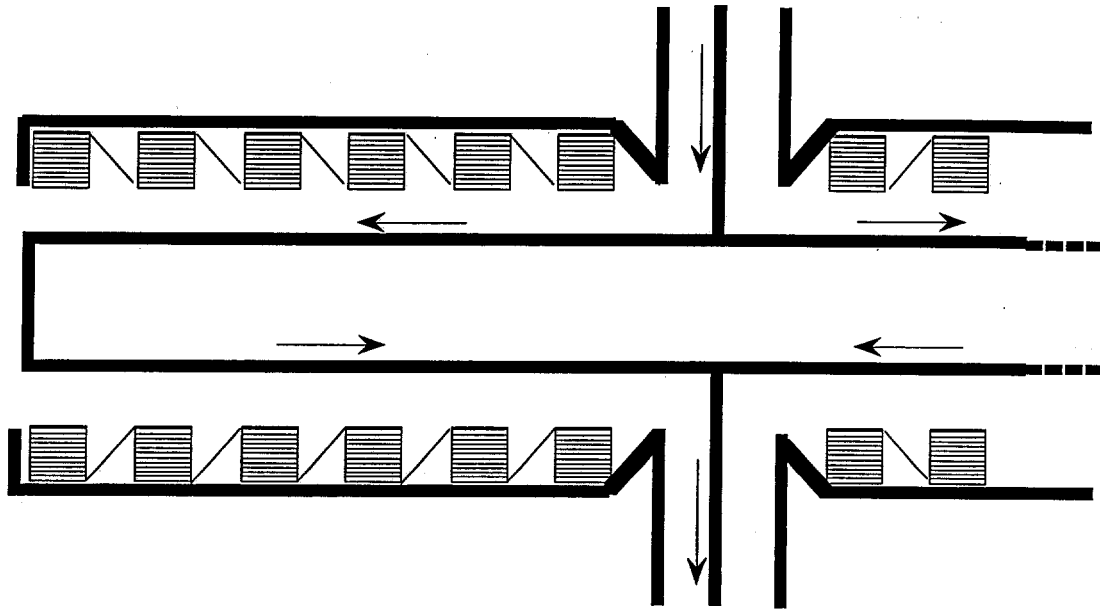


Figure 5. Partial side view of a magnet, showing magnetic cores, direction of current flows, and grounded shield surrounding the structure.

For this example, the requirement on the third-harmonic component of the shape of the windings is that it be less than 7% of the fundamental, to keep the third harmonic of the field on the 11-mm-radius circle below 3%. A third harmonic of this level may be the smallest practically achievable, since the current distribution wobbles on the surface of the conductors during the cycle. There is a second-harmonic components for skew fields (at times other than $\theta=0$ or multiples of 45°). However these components are canceled out by the symmetry of the 360° twist. Requirements on higher harmonics are fairly loose.

3-Phase Magnet.

Field distributions for a 3-phase magnet are shown in Figure 6. It is immediately clear from a comparison with Figure 1 that the field uniformity in the central region is greatly improved in the 3-phase magnet. The general design approach used for the 2-phase magnet continue to hold true for the 3-phase magnet. The windings can be constructed as in Figure 2, with the exception that the windings are separated azimuthally by 60° instead of 90° . The magnetic fields from adjacent conductors couple into each other, but the total magnetic coupling is in phase with the current/voltage of the conductor, such that, for a properly balanced system, the power supplies continue to see a purely inductive load. A POISSON calculation yields, for

the same dimensions as for the 2-phase magnet, a current of 1668 A for a field on axis of 880 G. The single-turn inductance is 0.992 μH . After accounting for the factor $4/\pi$ from the twist, the power supply current and voltage are 4248 A and 4137 V. The peak voltage with respect to ground is ± 2.1 kV, and the peak voltage difference between neighboring conductors is also 2.1 kV, over an 11.5-mm air gap.

For the 3-phase magnet the windings overlap such that the current for all 3 phases appears at a given angle. Since 3 phases can be synthesized from 2, it is in principle only necessary that the windings extend for 120° , not 180° as in Fig. 3. The reduction in twist reduces requirements on the power supplies by about 10%. Thus the numbers quoted for the 3-phase magnet voltage and current are conservative.

Conclusions.

Some parameters relevant to all the magnet designs considered here are listed in Table I. The requirements on the power supply for the rotating-field magnet (2-phase: 6 kA, 5 kV, 3-phase: 4 kA, 4 kV) are smaller than for kicker-type magnets. It is possible that careful refinements to shape and position of the conductors will further reduce the requirements on the power supply, after more detailed field calculations become available. For comparison, a kicker-type sweep magnet pair based on ferrite cores at 3-cm radius had a power supply requirement of 8 kA and 6 kV [Ref. 2]. A more recent design based on iron laminations that are very close to the beam required 5 kA and 6 kV. A kicker design based on tape-wound cores, with similar dimensions to those discussed above for the rotating-field magnet, would have a requirement between these two (7 kA, 6 kV). Plots from POISSON used to arrive at these numbers are attached (Figures 7-11).

The longitudinal electric field at the core is essentially the same as that along the conductors, neglecting any effect of the twist, because nearly all the flux returns through the core. The windings/laminations normally have only a thin oxide layer as insulation, and breakdown strength per lamination is expected to be quite low. The voltage per lamination should be kept as small as possible.

Table I

Magnet	Current	Voltage	eff len	length	L	V/gap	V/turn
3-phase	4 kA	4 kV	50 cm	56 cm	0.25 μH	160 V	0.32 V
2-phase	6	5	50	56	0.20	190	0.38
kicker-laminations	5	6	22	28	0.33		0.76
kicker-tape wound	7	6	22	28	0.22	250	0.5
kicker-ferrite	8	6	22	28	0.20		

This investigation shows that the rotating-field concept is a viable candidate for the sweep magnet. It reduces power supply requirements, and has lower induced electric field at the core. In view of the expected great difficulty and expense involved in stacking 10,000 laminations for each kicker-type magnet, the effective use of tape-wound cores is a great design advantage. Further work will be required to verify the calculations presented here, and to complete the engineering design. From a programmatic point of view, we may initially build a prototype 2-phase magnet, and only later build a 3-phase magnet, which is more complicated both electrically and mechanically. Because of its greater field uniformity and lower operating voltage, a 3-phase magnet could provide an upgrade path to larger sweep radius as beam intensity increases.

References.

1. Tyn Myint-U, Partial Differential Equations of Mathematical Physics, Elsevier, 1973, p. 209.
2. F. M. Bieniosek, A Beam Sweeping System for the Fermilab Antiproton Production Target, FNAL-TM-1857 (1993).

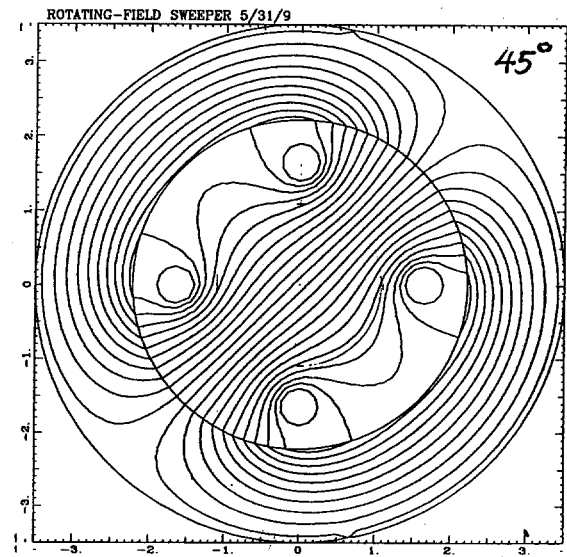
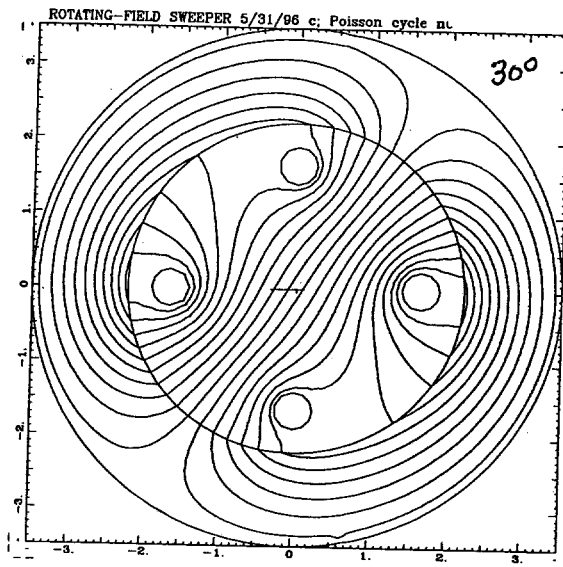
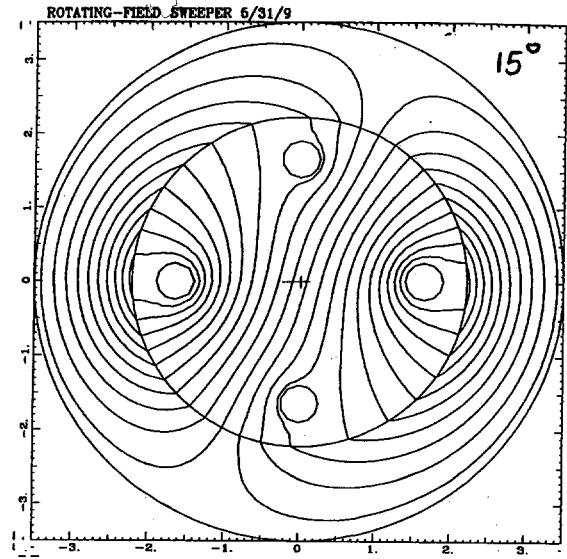
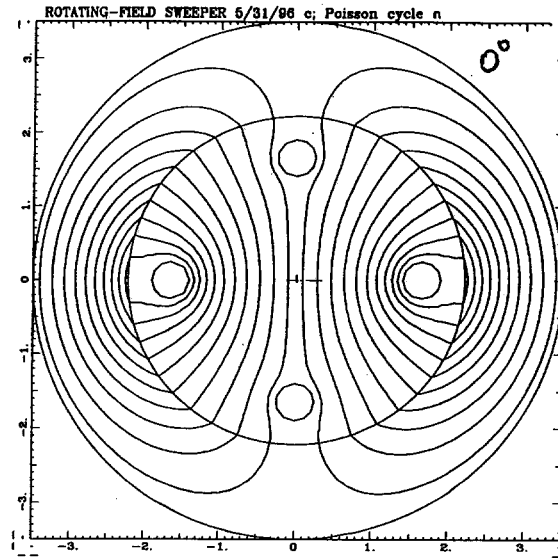


Figure 1. Local magnetic field structure for a 2-phase rotating-field sweep magnet. Current to horizontal pair of conductors has a $\cos(\omega t)$ time dependence; current to vertical pair of conductors has a $\sin(\omega t)$ time dependence. Field distribution is shown for (a) $\omega t=0$, (b) $\omega t=\pi/12$, (c) $\omega t=\pi/6$, (d) $\omega t=\pi/4$. A magnetic core surrounds the conductors. Dimensions are in cm.

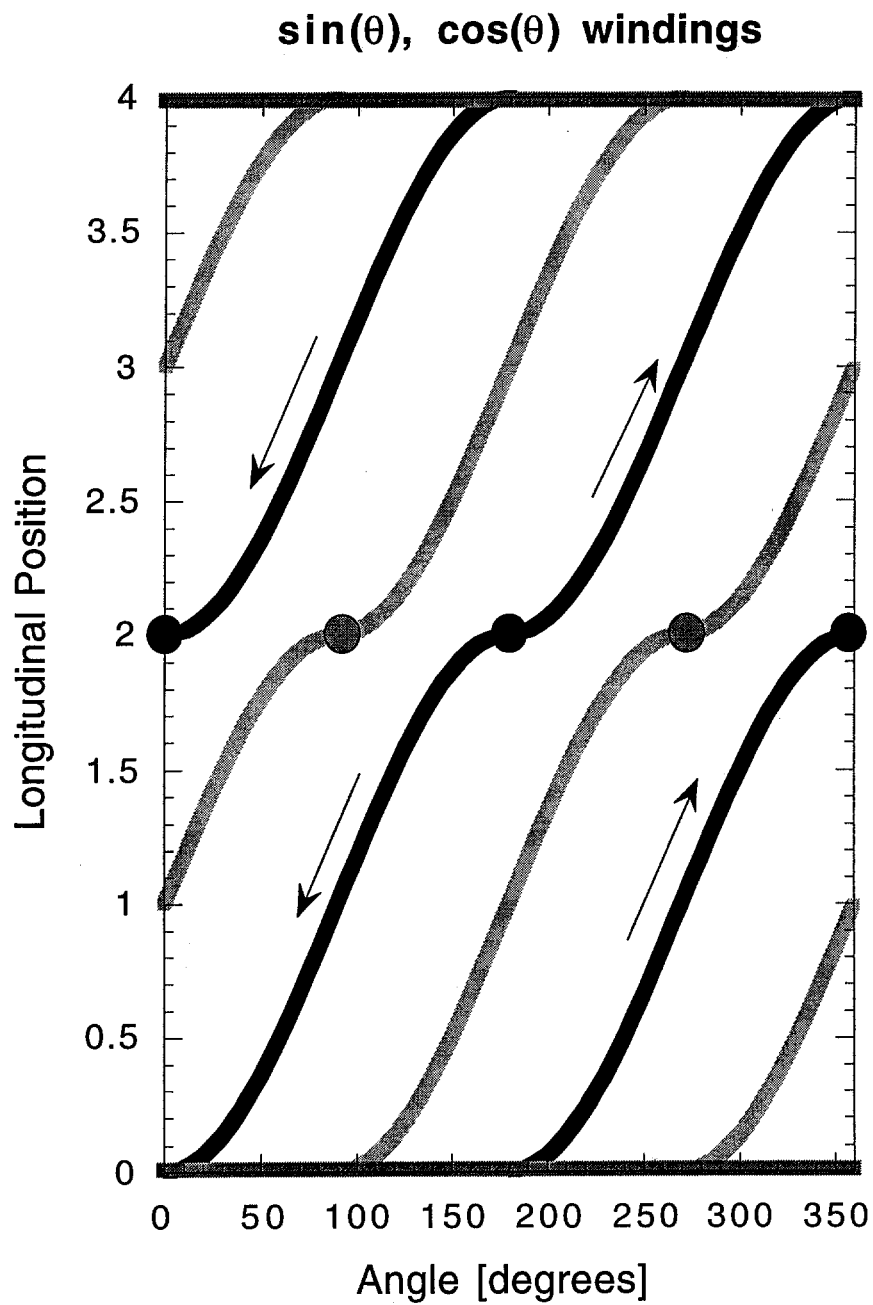


Figure 2. Shape of windings as a function of azimuthal angle for the 360° winding. The black curves represent one circuit, the gray curves represent the orthogonal circuit. Direction of current flow is indicated in one of the circuits.

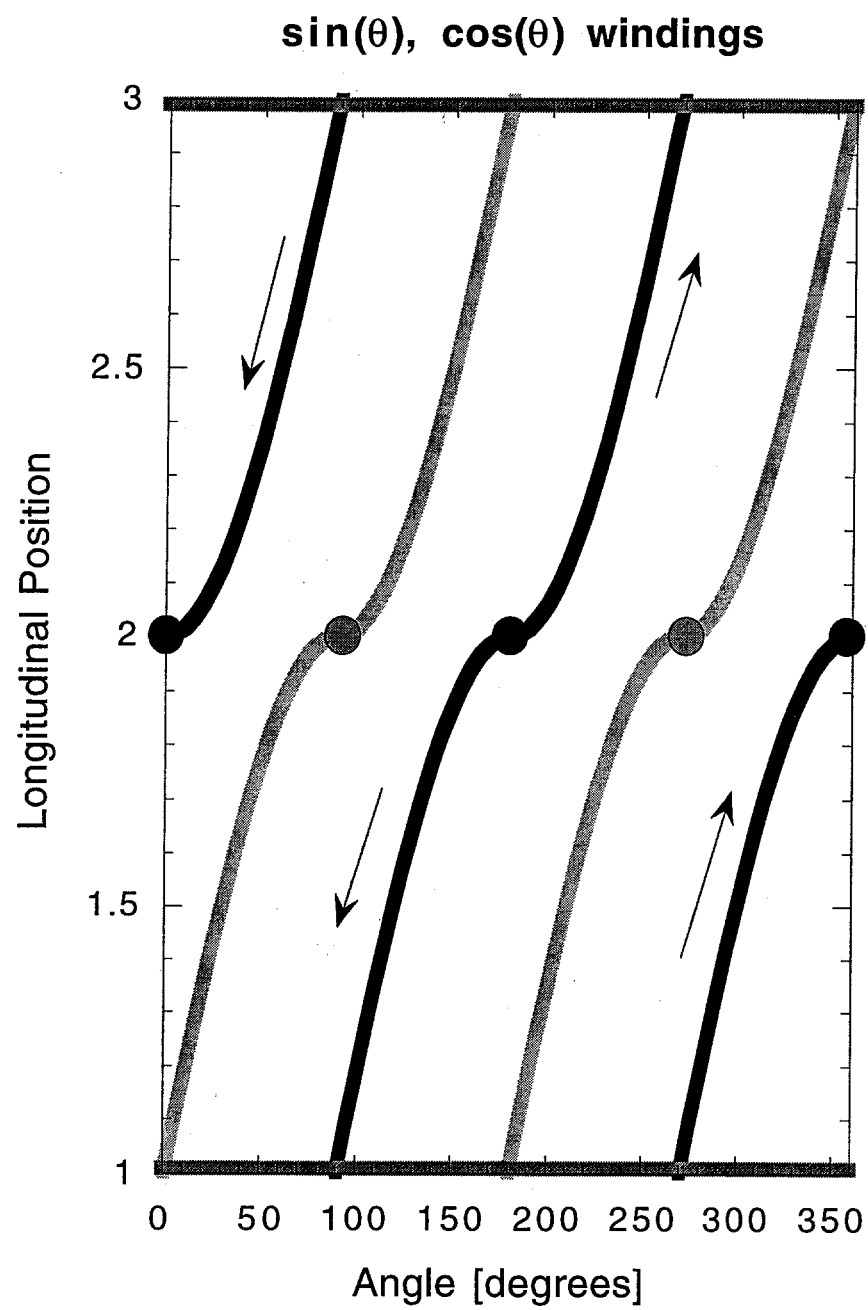


Figure 3. Shape of windings for the 180° winding.

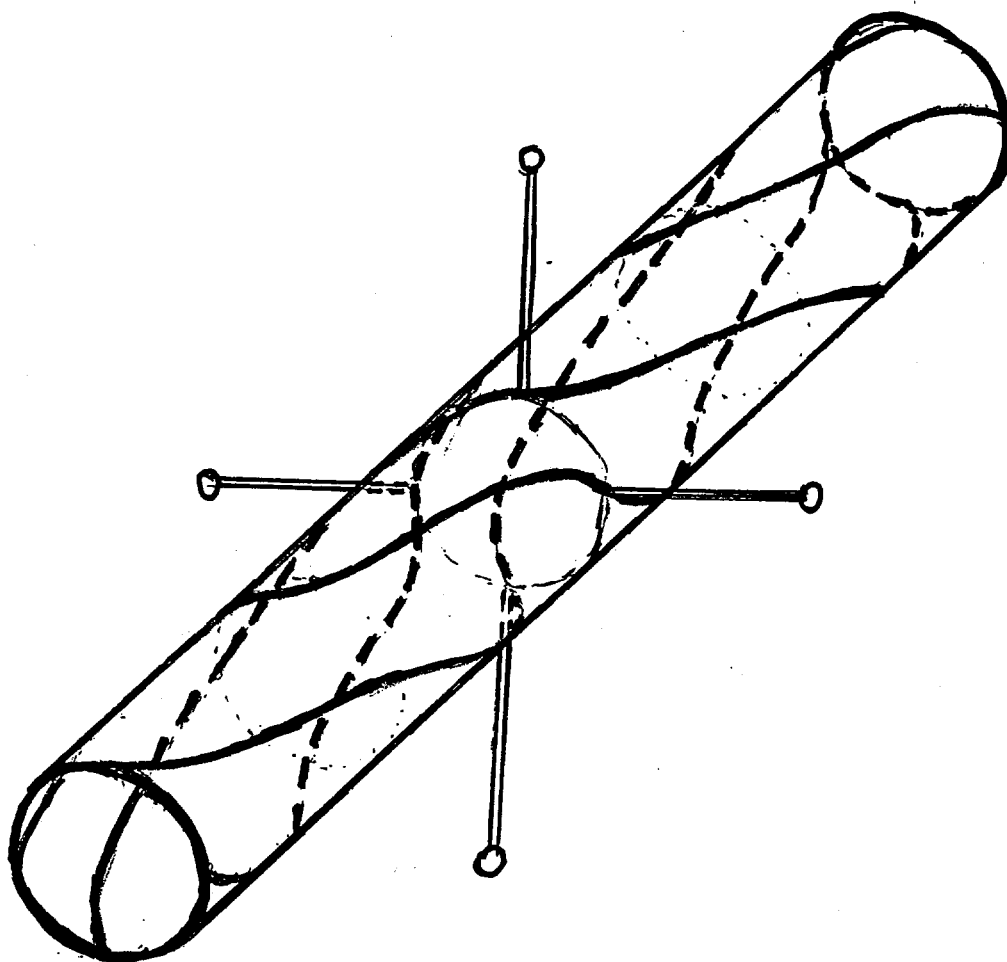


Figure 4. A 3-dimensional representation of the windings. The current for one circuit is supplied vertically; the current for the other circuit is supplied horizontally.

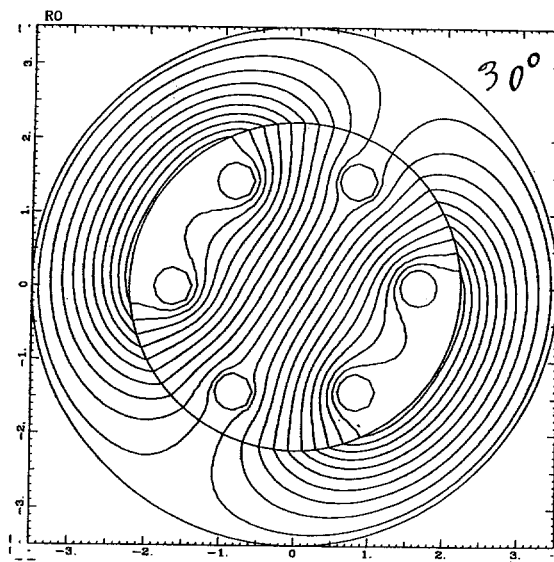
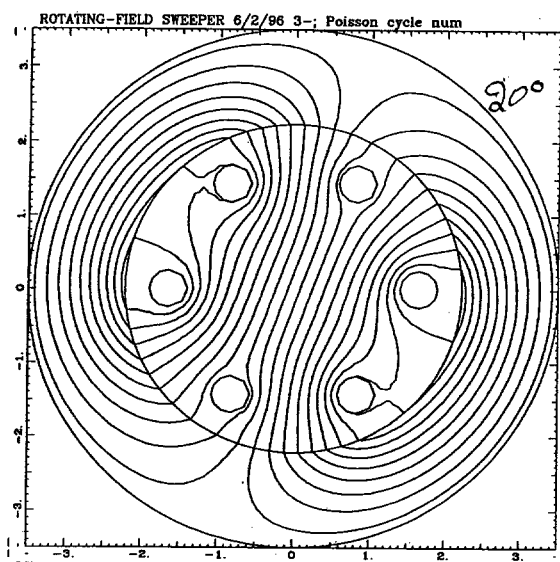
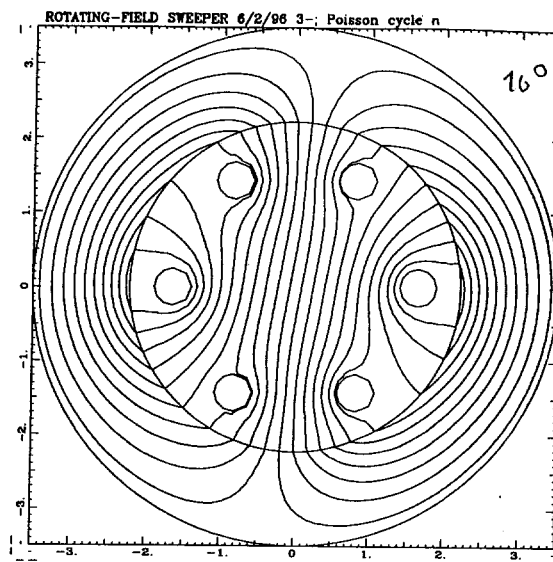
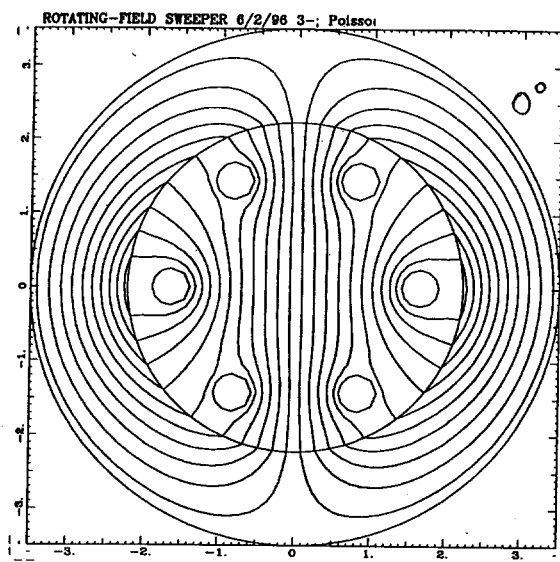
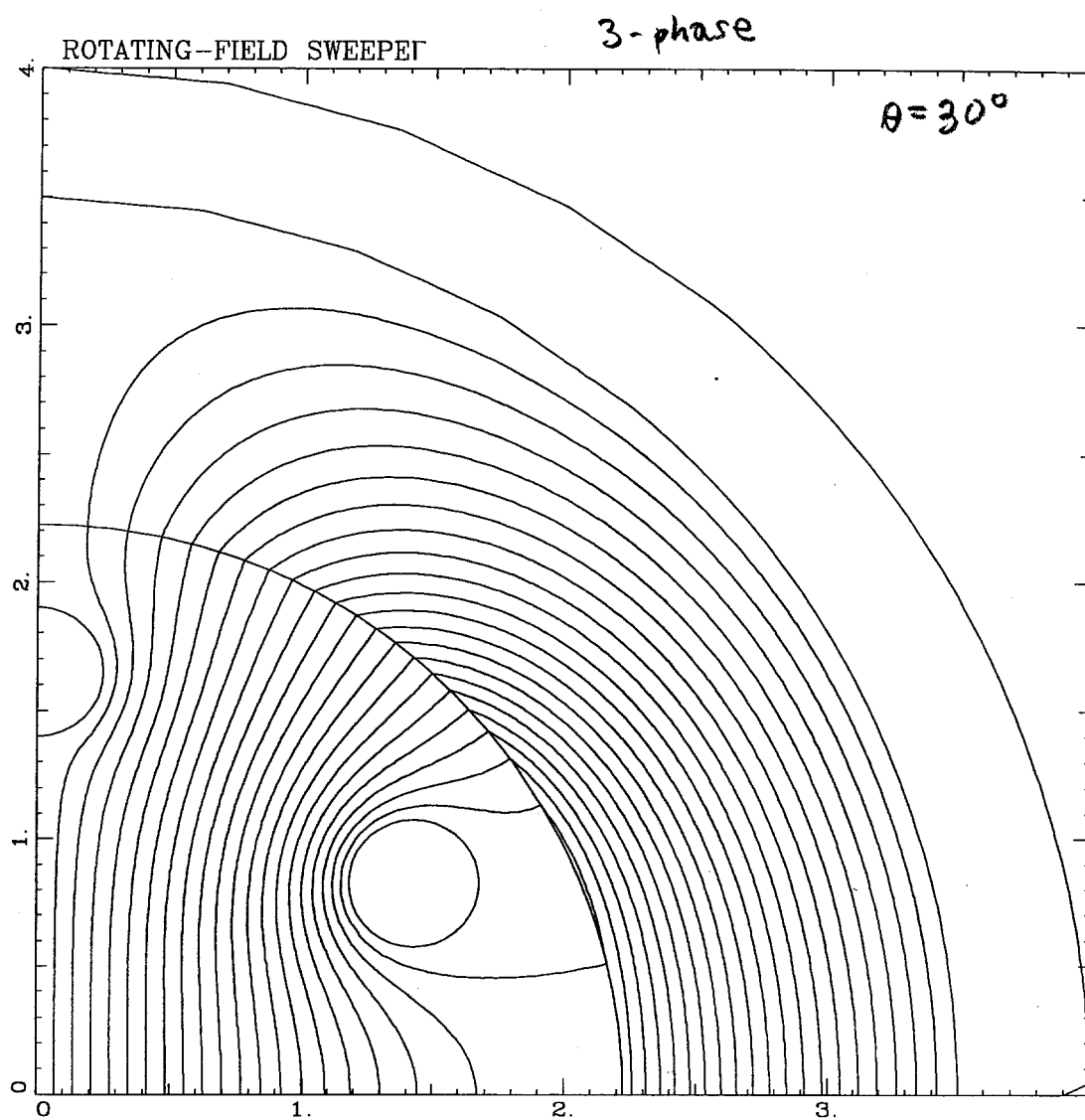


Figure 6. Local magnetic field structure for a 3-phase rotating-field sweep magnet. Field distribution is shown for (a) $\omega t=0$, (b) $\omega t=\pi/18$, (c) $\omega t=\pi/9$, (d) $\omega t=\pi/6$.



$$I_- = -3282 \text{ A}$$

$$I_t = 1210 \text{ A}$$

$$W = 4.771 \text{ J/m}$$

$$b_1 = -1999$$

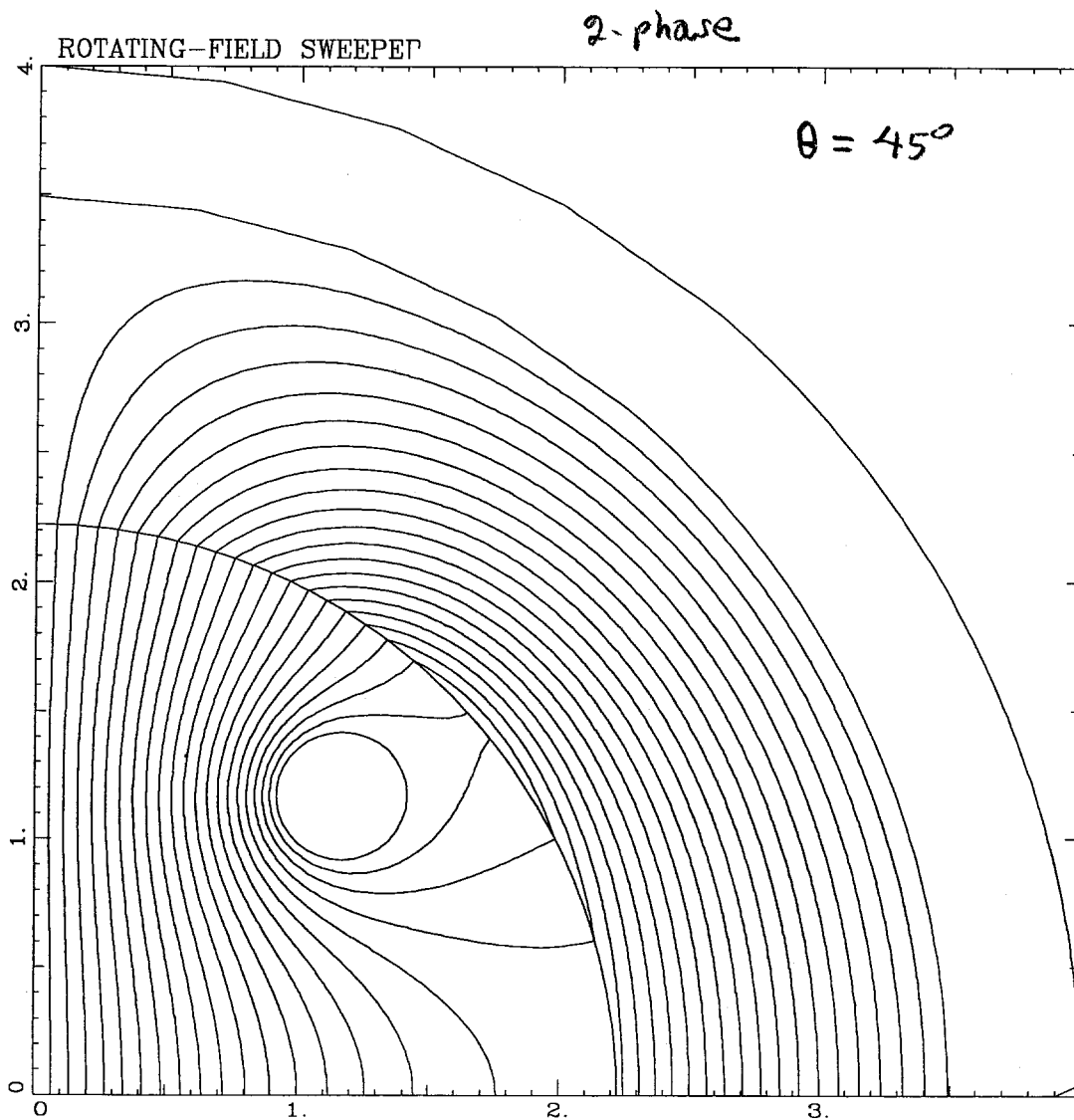
$$b_3 = -9$$

$$b_5 = 471$$

$$b_7 = 79$$

$$b_9 = -3$$

} harmonic analysis
on 1.1-cm
circle



$$I = -3872 \text{ A}$$

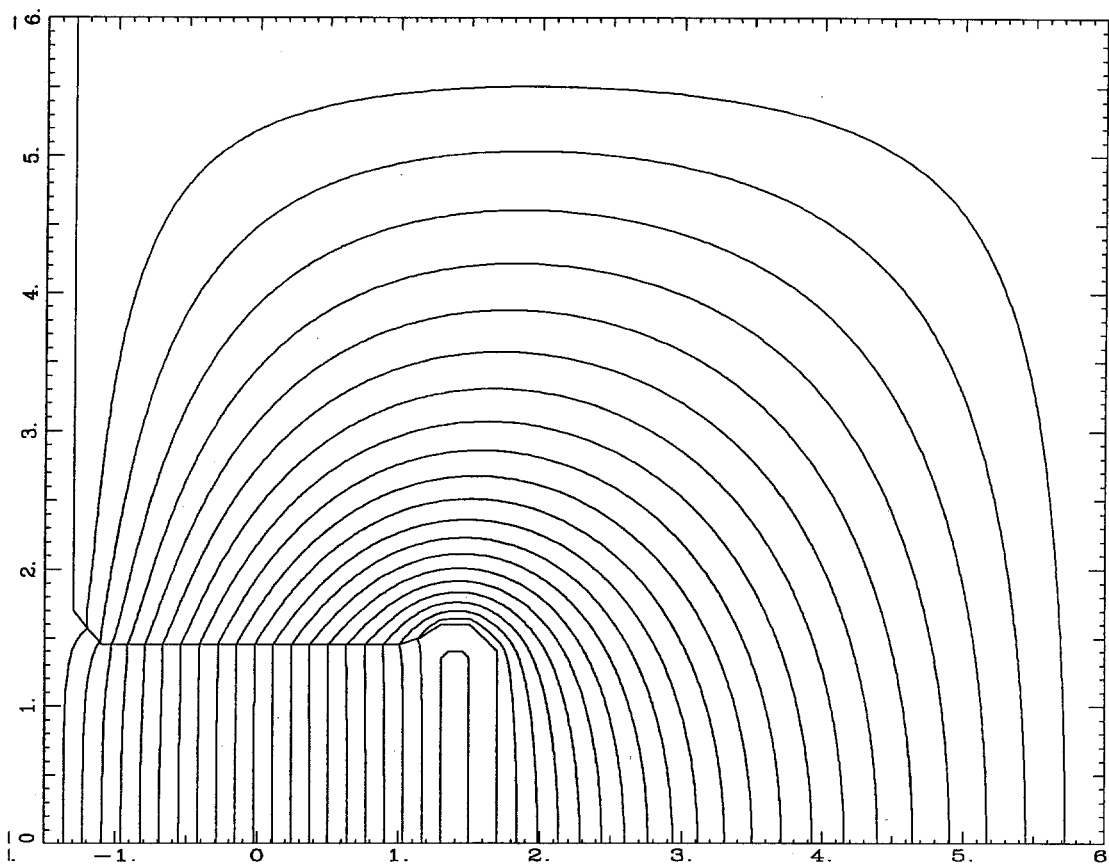
$$W = 5.472 \text{ J/m}$$

$$\left. \begin{aligned} b_1 &= -2002 \\ b_3 &= 823 \\ b_5 &= 259 \\ b_7 &= -183 \\ b_9 &= -141 \end{aligned} \right\}$$

harmonic analysis
on 1.1-cm
circle

kicker, lamination

INDUCTIVE DS MAGNET 2/10/95 ; Poisson cycle number



$$I = -2339 \text{ A}$$

$$W = 6.79 \text{ J/m}$$

$$b_1 = -2048$$

$$b_3 = 25$$

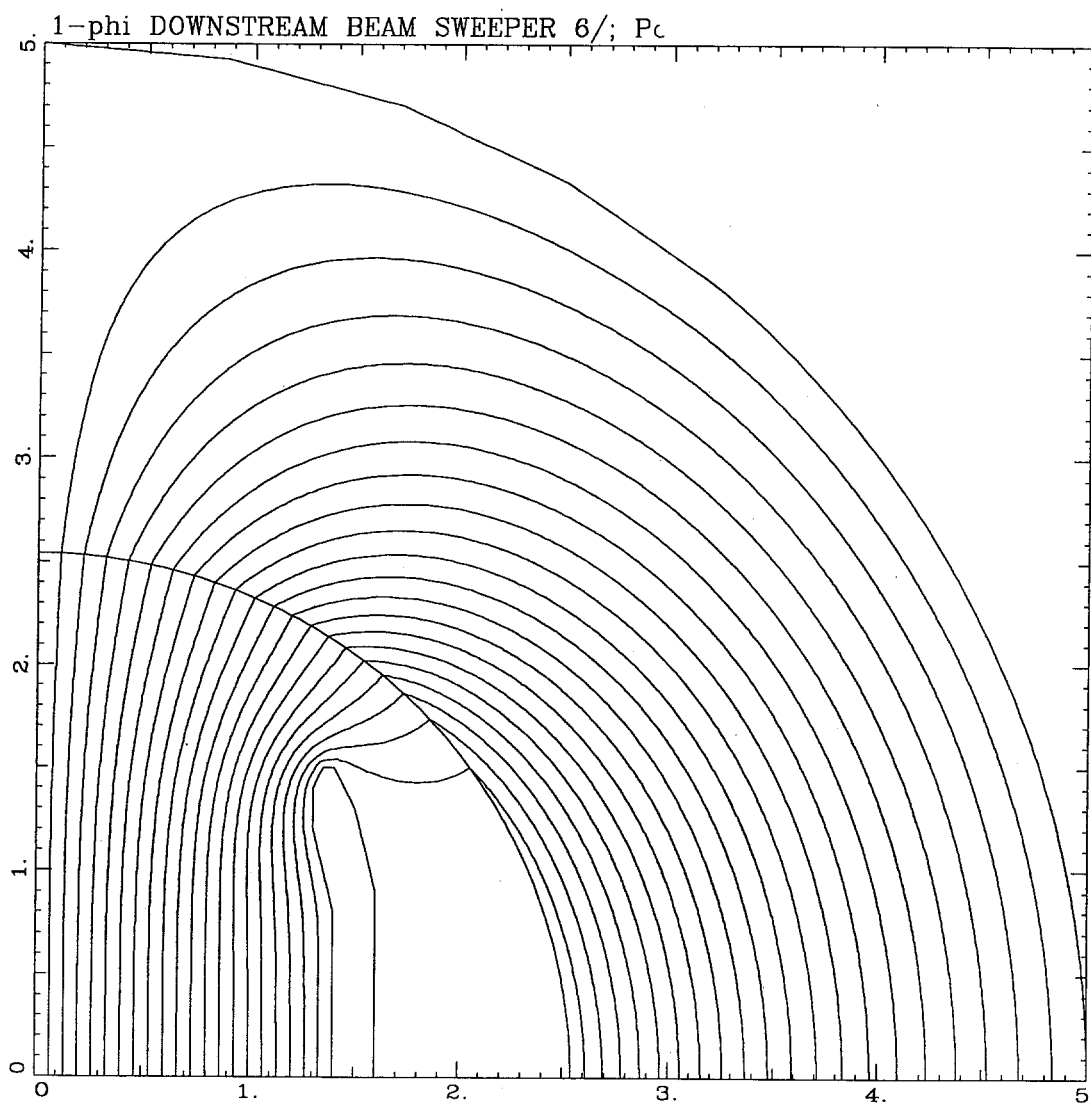
$$b_5 = -2$$

$$b_7 = -4$$

$$b_9 = 2$$

} harmonic analysis
on 1.1-cm
circle

kicker, tape-wound core



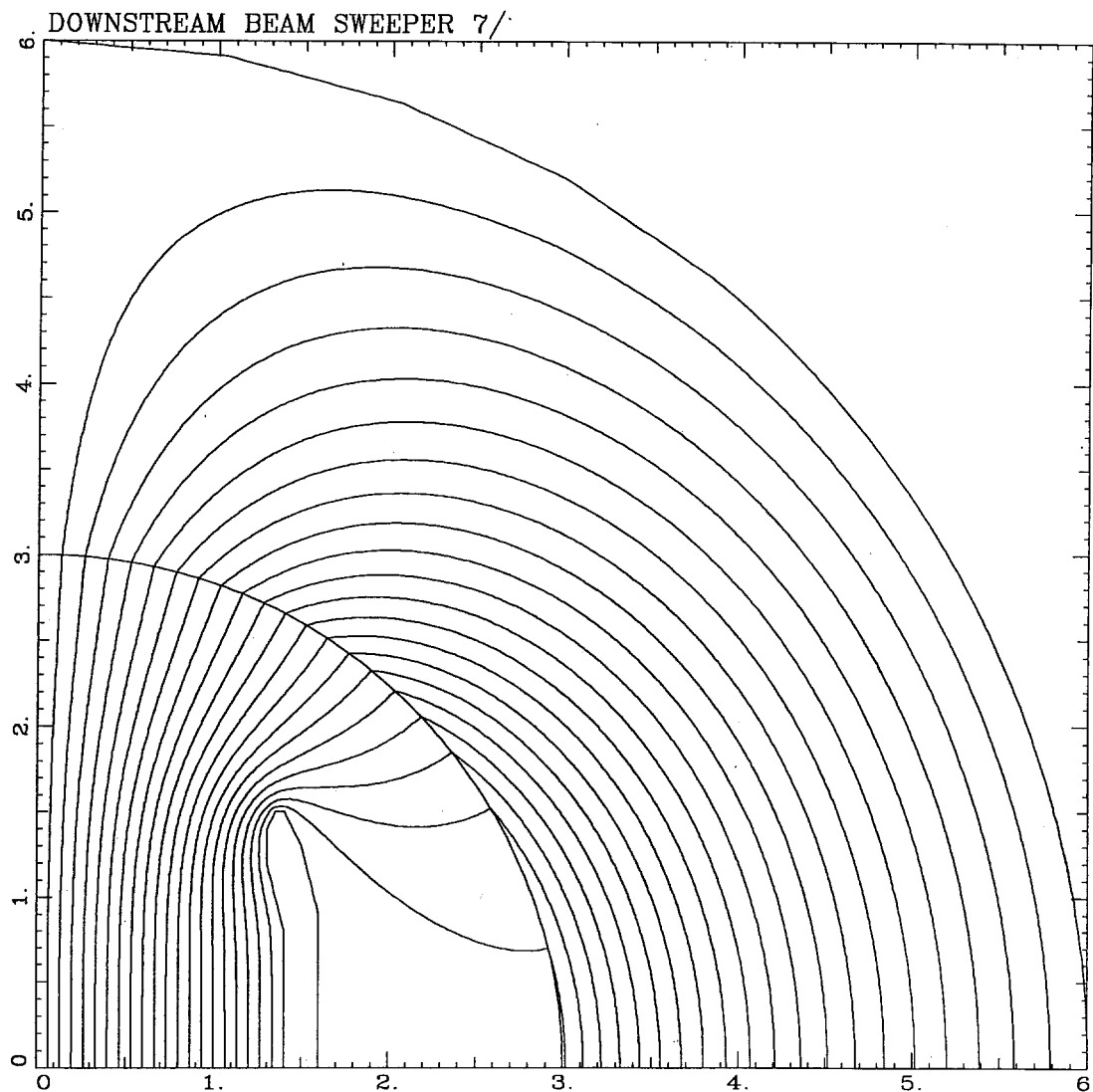
$$I = -3579 \text{ A}$$

$$W = 5.017 \text{ J/m}$$

$$\left. \begin{aligned} b_1 &= -2000 \\ b_3 &= -31 \\ b_5 &= 51 \\ b_7 &= -4 \\ b_9 &= -7 \end{aligned} \right\}$$

Harmonic analysis
on 1.1-cm
circle

kicker, ferrite



$$I = -3940 \text{ A}$$
$$W = 5.532 \text{ J/m}$$

$$\left. \begin{array}{l} b_1 = -2000 \\ b_3 = -41 \\ b_5 = +55 \\ b_7 = -4 \\ b_9 = -6 \end{array} \right\} \begin{array}{l} \text{harmonic analysis} \\ \text{on 1.1-cm} \\ \text{circle} \end{array}$$